JOURNAL OF CATALYSIS 41, 293–302 (1976)

Development of a New Isothermal Calorimeter; Heats of Hydrogen Adsorption on Supported Platinum vs Crystallite Size

JOEL B. LANTZ AND RICHARD D. GONZALEZ

Department of Chemistry, University of Rhode Island, Kingston, Rhode Island 02881

Received June 2, 1975

Heats of hydrogen adsorption over silica-supported platimun were measured calorimetrically as a function of dispersion. To measure the relatively small heats evolved, a sensitive calorimeter with a completely new type of detection system was constructed.

The initial adsorption heats in three Q vs θ plots obtained decreased slightly with increasing dispersion. In all three plots local maxima corresponding to $\theta = 0.4$ were observed. It was concluded that heats of adsorption are largely independent of dispersion. This is in agreement with the facile nature of most reactions over supported platinum.

INTRODUCTION

According to Taylor (*1*), atoms on corners, edges, and defects of a crystal and other areas of small curvature will bond with adsorbate molecules more strongly than will atoms on regular crystallographic planes due to their larger lattice coordination numbers. Poltorak and Boronin (*2*), have shown from geometric considerations that in an ideal platinum crystal, the number of edge atoms increases far more slowly than the number of face atoms as the crystal diameter increases (the number of corner atoms remains constant). At about 40–50 Å edge length, the face atoms heavily predominate. Because similar arguments apply to other metals, one should in general expect integral heats of adsorption (a direct function of the sum of individual metal–adsorbate bond energies) to decrease as the overall crystallite size of a metal catalyst increases.

According to the Taylor (*1*) hypothesis, incoming adsorbate molecules should fill the surface in order of decreasing site energy. This behavior is often used to partially explain the decreasing heats of adsorption observed with increasing fractional surface coverage for various adsorbent/adsorbate systems. Adsorption on edges, corners, defects, etc., of crystallites should therefore correspond to low surface coverages in differential adsorption–heat plots. Decreases in the adsorption heat due to increasing crystallite size and a corresponding decrease in the proportion of such most energetic sites should also occur at low surface coverages.

Surprisingly, the great majority of studies involving catalytic hydrogenations over supported platinum have been shown to be facile [a term coined by Boudart (*3*) to group together those reactions for which specific activity is insensitive to dispersion]. Exceptions (*4*) usually involve larger organic molecules which interact with the surface in a more subtle way. This insensitivity to dispersion may in part be due to the high mobility displayed by hydrogen over platinum; i.e., the hydrogen atoms could conceivably be formed at edges and corners and rapidly migrate to the less

energetic sites on the crystallite faces. This would tend to obscure dispersion effects on specific activities.

Systematic studies on heats of adsorption as a function of dispersion are generally lacking in the literature. Recently, Van Hardeveld and Van Montfoort (*5*) have shown that isosteric heats of nitrogen adsorption over supported nickel depend on dispersion. They attributed the higher heats of adsorption obtained for the small crystallites to a special kind of adsorption site (B5), at which a molecule can coordinate with five metal atoms. Although their envisionment of these high-energy sites is somewhat different from that of Taylor, it is complementary. It is not clear from their work whether the nitrogen was chemically or physically adsorbed, however.

Heats of adsorption for hydrogen on the relatively large crystallites of platinum black have dominated the literature. Such investigations on silica-supported platinum are few, and none of these are calorimetric. The initial heats reported for hydrogen on platinum are extremely variable from author to author, as are the shapes of the heat of adsorption curves. Virtually none of these studies, save perhaps one, represents a systematic investigation of adsorption heat vs dispersion.

The lone exception, an isosteric study by Boronin, Nikulina, and Poltorak (*6*) on platinum crystallites of three different sizes (8, 10–20, and 100–200 Å), does not include data in the region below 20% surface coverage where, according to Bond (*7*), these effects, if any, should be observed. Although there is a single point at 20% surface coverage, most of their comparative data are for surface coverages in excess of 50%.

Isosteric heats calculated from the Clausius–Clapeyron equation are not reliable unless the adsorbate is reversibly and homogeneously adsorbed, a requirement that is certainly not met in the chemical adsorption of hydrogen on platinum. In spite of the difficulties involved in accurate calorimetric measurements, results obtained in direct calorimetric measurements are much more reliable than those derived from indirect thermodynamic calculations. It is for this reason that this study was undertaken. Accurate calorimetric measurements on supported metals as a function of dispersion are needed to fill an important gap in the catalytic literature.

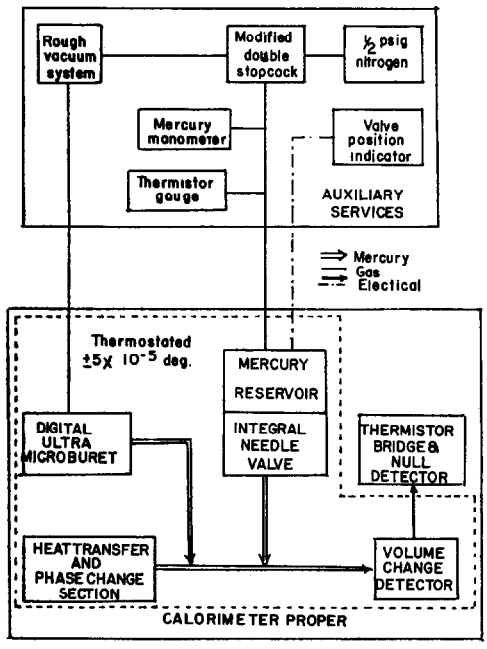

FIG. 1. Calorimeter system, block diagram.

EXPERIMENTAL

Calorimeter. An isothermal calorimeter was used for measuring the adsorption heats. This instrument, which utilized a unique detection system, is outlined in the system block diagram, Fig. 1. The parts, which were surrounded by a precision constant temperature bath, are shown in the pictorial schematic, Fig. 2.

Melting of a frozen phenyl ether mantle (in equilibrium with the liquid) around the reaction chamber, via a heat transfer well (No. 9 in Fig. 2), produced a specific volume change and consequent mercury displace-

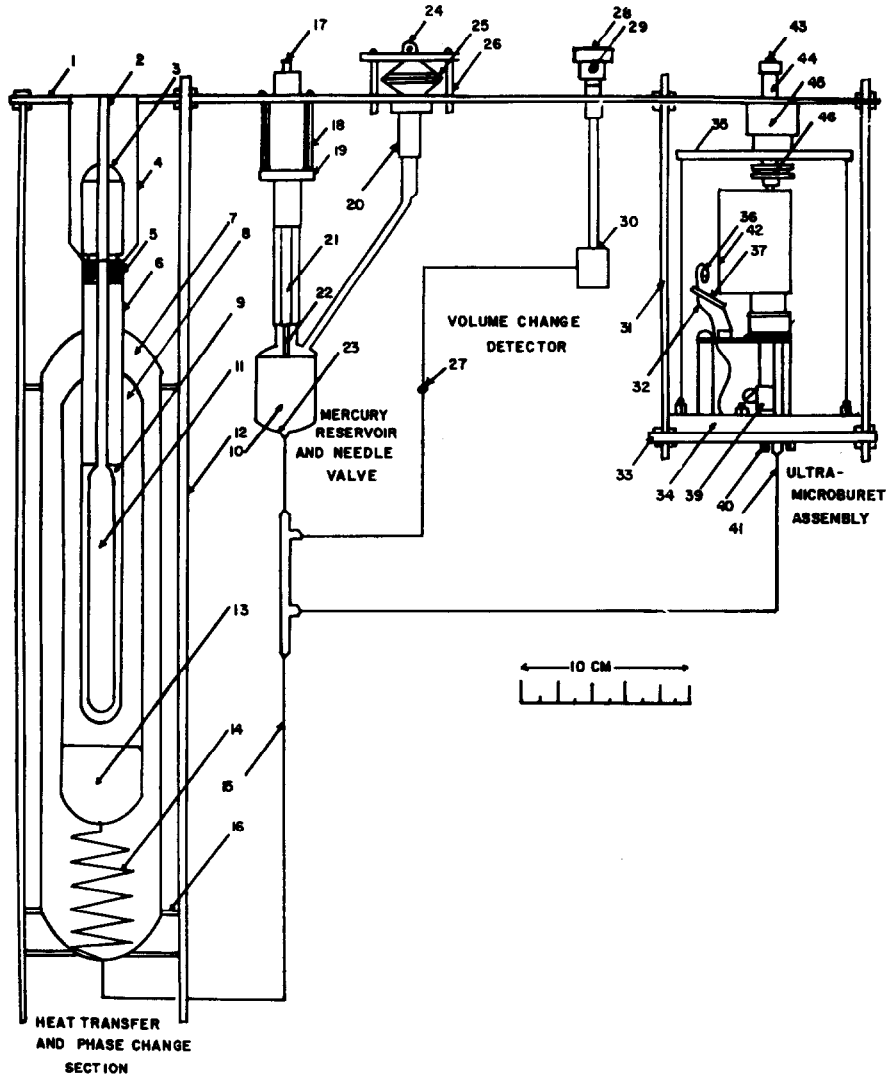

FIG. 2. Calorimeter proper, schematic front view. *1*, Aluminum mounting plate; *2*, connection to vacuum line; *3*, 29/42 standard-taper joints; *4*, heat-exchange sleeve and brass extension tube; *5*, thermal shunt; *6*, flex coupling; *7*, vacuum jacket; *8*, ether chamber; *9*, heat-transfer well, showing fluid; *10*, mercury; *11*, catalyst; *12*, threaded stainless-steel rod; *13*, mercury; *14*, 2 mm i.d. capillary; *15*, 1.5–2 mm i.d. capillary used throughout, except in detector; *16*, stainless-steel support rings (3), with vinyl pads; *17*, valve adjustment screw; *18*, mounting screws; *19*, valve mounting, transport, and shift-sealing assembly; *20*, mounting flange for O-ring joint; *21*, stainless steel shaft; *22*, nylon shaft; *23*, valve seat; O-ring on tapered tip of shaft (not shown) seals here; *24*, connection of mercury reservoir to auxiliary services; *25*, O-ring joint; *26*, screw-down clamping assembly; *27*, safety bulb; *28*, moisture-resistant electrical connection chamber; *29*, wire leads out to thermistor bridge; *30*, detector (see also Fig. 1); *31*, threaded stainless-steel rod; *32*, electrical wires to lamp; *33*, stainless-steel plate; *34*, Plexiglas O-ring flange; *35*, clear plastic buret tank; *36*, AlC neon lamp (high brightness); *37*, front-surface mirror; *38*, buret mounting collar and clamping screw; *39*, compression seal; *40*, feed-through seal; *41*, displacement-tube assembly; *42*, ultramicroburet (arrow points to readout window); *43*, screwdriver adjustment fitting; *44*, stainless-steel shaft; *45*, O-ring seal and thrust bearing, *46*, mechanical linkage.

ment. This displacement was measured by a variable-resistance detector and its associated bridge circuit. The detector was normally calibrated with added displacements of an ultramicro-buret over a 40 μl range, corresponding to 10 cal. Careful adjustments of initial displacements in the detector were possible by pressurizing a mercury reservoir with nitrogen to a few Torr above or below the effective mercury head at the detector level and regulating its flow to or from the detector with the needle valve. Auxiliary services provided the necessary gas and vacuum for these adjustments and also provided a vacuum behind the piston seal of the ultramicro-buret via a tank surrounding it (and thereby prevented air from entering the system, which operates at subambient pressure). The dead space in the mercury reservoir, in combination with a high-pressure thermistor gauge, served as a crude volume-change detector during mantle formation.

The detector was an air-filled (1–2 Torr) microvolume thermistor gauge that responded to very small volume changes. It was composed of a 14 ml thermistor bead sealed into a tiny borosilicate glass bulb by a technique based on that of Bradley (*8*), combined with a sintered-glass protective fill. The internal volume varied between roughly 50 and 90 μl over the usual calibration range. The thermistor was one arm of a balanced bridge circuit that was powered by an isolated, high-precision voltage supply to ensure reproducible heating of the thermistor. Practical resolutions from 250 to 80 μcal could regularly be obtained over the 10 cal calibration range used during the adsorption experiments. The displacement calibration was in the form of the polynomial

$$V = a + b\,(R - 1500) + \cdots + e\,(R - 1500)^4,$$

where R is the detector resistance, in ohms, and V is the displacement in microliters. The constants, which were determined via a least-squares analysis of the calibration data, were, for a typical calibration $a = 7.7504$, $b = 0.17974$, $c = 2.7612 \times 10^{-4}$, $d = 2.6842 \times 10^{-7}$, and $e = 1.1417 \times 10^{-10}$. The evolved heat was calculated (after appropriate corrections for calorimetric drift) from

$$Q = k\,(V_{\text{initial}} - V_{\text{final}}),$$

where $k = 0.2562$ cal/μl, based on the average of four calibration factors listed by Jessup (*9*).

The entire assembly in Fig. 2 is immersed in a water bath (to a level just below the top of the tank No. 35). The temperature of this bath was maintained almost at the phenylether triple point to minimize calorimetric drift rate (ca. 26.9°C). Regulation was possible to better than ± 50 μdeg over several hours corresponding to a calorimetric drift uncertainty of ± 120 μcal/min. A sensitive control system and thermostated barriers between the room and the primary insulation layers around the tank made this control possible despite serious ambient temperature control problems. The thermal barrier temperature was adjusted to compensate for kinetic heat input from the stirrer. Minor changes in heat flux could conversely be compensated for by adjusting the stirrer speed.

The temperature control system was basically a thermistor probe/dc bridge/control relay combination. A temperature deviation unbalanced an isolated dc bridge. The unbalanced signal, after passing through an ultralow drift, high-gain amplifier, triggered a sensitive relay/triac to power the bath heaters. A very low power heater wound around the thermistor probe created a time-proportioning effect, based on the variation of the rate of heat removal from the probe with temperature [see (*10*)].

In relatively crude heater calibrations, the accuracy and precision appeared to be 0.030 cal or 1%, whichever was greater. This figure is two orders of magnitude larger than the sensitivity, and was thus disap-

pointing. Inaccuracies in the applied heat values and in the ultramicroburet doubtless contributed to these deviations. Further details regarding the calorimeter have been published elsewhere (*11*).

Materials. The phenylether (reagent grade obtained from J. T. Baker Chemical Company) was purified by repeated recrystallizations. The averages of three triple points each for the ether obtained from recrystallizations No. 4 and No. 5 were approximately 0.001°C apart (actually 0.0013°C), a temperature spread which Dainton (*12*), in the case of freezing points, considered to represent an adequate purity for the contents of his precision calorimeter. Regardless, the phenylether was recrystallized a sixth time before filling the calorimeter.

Hydrogen (research grade, 99.993% purity) and helium (research grade 99.9999%) were obtained from the Lif-o-Gen Corporation, Cambridge, Maryland. They were not submitted to further purification. The silica gel used was Davidson Grade 62 (donated by the W. R. Grace Company, Balto, Maryland). Physical characteristics as listed by the manufacturer are 1.16 cm^3/g pore volume, 1.40 Å average pore diameter, 340 m^2/g surface area and 60–200 mesh particle size.

Preparation of the unreduced catalyst. The preparation of the catalyst was based on the method of Boronin *et al.* (*13*). Catalysts with extremely small average crystallite size (ca. 10 Å) were obtained by these authors by adsorbing a platinum–ammine chloride complex onto the silica and then reducing it in hydrogen at a very low static pressure (0.1–1 Torr). When careful attention was paid to details in the preparation of such catalysts, the average particle sizes were largely independent of the platinum content.

A platinum–ammine chloride solution was prepared by first dissolving 4.0 g of chloroplatinic acid in 100 ml of doubly distilled water in a 250 ml volumetric flask. After heating this solution to 80–90°C., 32.5 ml of concentrated ammonium hydroxide were added. The solution was maintained at 80–90°C for 20 min and cooled, after which the flask was filled to the mark with doubly distilled water and shaken well. This is not a solution containing $Pt(NH_3)_4^{2+}$, as implied by Dorling *et al.* (*14*), but a mixture of $Pt(NH_3)_5Cl^{3+}$ and $Pt(NH_3)_6^{4+}$, as indicated by Kung *et al.* (*15*). The Davidson Grade 62 silica gel was chosen over fumed silica due to its better thermal conductivity properties.

Before treatment with platinum–ammine solution, 24 g of the silica was placed in a long glass tube and heated in oxygen at 330°C for several hours to oxidize any hydrocarbons that may have been adsorbed during storage. After baking the oxygen off in vacuum, the ammine solution was admitted to the tube through a Teflon and glass vacuum valve. The tube was then sealed and rotated horizontally about its axis for several days to effect agitation. It was stored under vacuum until further use.

Reduction of the catalyst. An 8.15 g sample of catalyst was charged to the reaction tube (No. 11, Fig. 2). The reaction tube was made from 19 mm o.d. tubing (Vycor glass up to just inside taper joint No. 3, where a transition to borosilicate glass occurs). The catalyst was dried in air at 60–70°C for 3 hr and heated slowly in air to 130°C. The air was then evacuated and the catalyst was heated slowly to 290°C, at which temperature the platinum–ammine rapidly began decomposing. Evacuation was continued until the pressure was reduced to the micron range. The catalyst was then reduced in hydrogen (left over from the previous run) at 485–495°C and evacuated for 3 hr at the same temperature. After each heat treatment, small amounts of ammonium chloride apparently were evolved and hence it was regarded as a possible contaminant. It would have been impossible to remove all of the ammonium chloride from the catalyst without consider-

able heat treatment and consequent sintering. The final heat treatment was at 550C° for 26 hr following a 7 hr evacuation at the same temperature. After this pretreatment, additional hydrogen was added, the temperature was reduced to 490°C, and an evacuation was carried out as in prior runs.

Determination of the adsorption heats and platinum surface areas. A typical run consisted of obtaining adsorption heats over eight to ten additions of hydrogen to the catalyst. Each gas addition in run No. 1 generally corresponded to 10–15% of the total platinum surface. The first four additions of gas in run Nos. 4 and 5 generally corresponded to 5–7% of the total surface to obtain better characterization of the important region of initial surface coverage. Each run was started by outgassing, as previously described, and then equilibrating the catalyst at a temperature somewhat below 26.9°C. The equilibration took about 2 hr due to the rather poor thermal conductivity of the catalyst. The reaction tube was then mated to the calorimeter, the top layers of insulation were installed, and the adsorption heats were measured. Calorimetric drift rates were established before and after each dose of hydrogen was adsorbed.

The adsorption process was quite slow for the last segment or two of each run, sometimes requiring several hours. Poor thermal conductivity was partly responsible for long experiment times. The heat transfer limitations, also responsible for long equilibration times, were somewhat circumvented through the addition of 0.1–0.2 Torr of helium to aid in heat transfer within the catalyst.

Determination of platinum surface area. The total platinum surface area of the catalyst was determined immediately after the calorimetric part of each run by adsorbing hydrogen on the remaining surface of the catalyst at −63°C. Although chemisorption measurements have long been used to measure the surface area of an adsorbent, no agreement exists concerning the criteria for monolayer coverage. Such measurements have been made with hydrogen on platinum from −196 to 250°C, with various final pressures considered to represent full coverage. Vannice *et al.* (*16*) have published

TABLE 1

Hydrogen Adsorbed during Each Run, after Various Heat Treatments of the Catalyst, and Corresponding Derived Measures of Platinum Dispersion

Run number	1	2	3	4	5
Heat treatment at 485–95°C after previous run (hr):					
In hydrogen	½[a]	½	½	½	26 hr at 550–55°C
In vacuum	10½[a]	3½	3½	3½	3½, plus 7 hr at 550–55°C
Total hydrogen adsorbed during entire run (mmol)	1.06	1.01	1.01	0.99	0.79
Uncertainty (mmol)[b]	±0.004	±0.004	±0.003	±0.004	±0.004
H atoms adsorbed/Pt atom in catalyst	0.83	0.79	0.79	0.78	0.62
Uncertainty[c]	±0.003	±0.003	±0.002	±0.003	±0.003

[a] Pretreatment of catalyst after initial reduction procedure.

[b] (Uncertainty)^2 = $\Sigma\Delta N^2$ (ΔN is the uncertainty in amount of hydrogen absorbed during each segment of an entire run.

[c] From uncertainty in total hydrogen adsorbed. Values are also all estimated to be high or low within 5.6%, twice the relative standard deviation of the platinum analysis, which was used in calculating all the H/Pt ratios.

TABLE 2

Adsorption and Calorimetric Data for Run No. 1

Adsorption temperature (°K)	Adsorption segment notation	Adsorption segment number	Equilibrium pressure, $P_{eq,m}$, $P_{eq,\theta}$, or $P_{eq,n}$ (Torr)	Amount of hydrogen adsorbed, N_m, N_θ, or N_n (μmol)	Uncorrected calorimeter displacement, $Dt - D_i$ (μl)	Average calorimeter drift rate, D (nl/min)	Thermal settling time, t (min)	Adsorption heat, Q_{ads} (kcal/mol)	Fraction of surface covered, θ_m
300	m	1	low	113.6 ± 0.4	10.07	2.54[a]	218	21.4[a]	0.107
300	m	2	low	119.2 ± 0.4	10.15	2.56[a]	168	20.9[a]	0.220
300	m	3	low	117.6 ± 0.4	9.76	2.56[a]	300	19.5[a]	0.331
300	m	4	low	124.2 ± 0.4	10.24	1.91 ± 0.63	300	19.9 ± 0.6	0.449
300	m	5	low	142.9 ± 0.5	8.81	1.51 ± 0.23	160	15.8 ± 0.4	0.584
300	m	6	0.7	144.4 ± 0.9	8.16	1.23 ± 0.51	200	14.1 ± 0.4	0.720
300	m	7	9.5	109.7 ± 1.0	4.90	0.30 ± 0.41	242	11.2 ± 0.6	0.824
300	m	8	44.2	64.8 ± 1.1	2.60	2.3 ± 1.0	64	8.8 ± 0.8	0.885
210	0	0	14.9	92.5 ± 1.2					
210	n	1	33.7	16.1 ± 1.5					
210	n	2	45.8	10.2 ± 2.0					
210	n	3	62.2	12.0 ± 2.5					

[a] Uncertainty is not known because drift rate had to be estimated.

a study in which the surface areas of platinum black obtained by hydrogen chemisorption agreed closely with those obtained by BET measurements for adsorption temperatures in the −60 to −80°C range and a final pressure of 50 Torr. In this work, a final pressure of 50 Torr at −63°C was taken as monolayer coverage.

Analysis of catalyst. The platinum content was obtained by vaporizing the silica support in concentrated HF and dissolving the platinum residue in aqua regia. A spectrophotometric technique was used to determine the platinum content.

RESULTS AND DISCUSSION

The results of the hydrogen adsorption measurements for the five runs and the dispersion parameters calculated from them are shown in Table 1. The initial dispersions were not as high as expected, probably due to pressure buildup during the decomposition of the platinum–ammine. Surface areas were calculated by the method of Spenadel and Boudart (*17*) by assuming that the crystallographic planes on the crystallite surfaces are 100 and 110, each having the same degree of exposure to the gas phase. The site densities on the surface are then 1.31×10^{19} and 0.93×10^{19} sites/m^2, respectively, yielding a mean of 1.12×10^{19} sites/m^2.

Plots of the heats of hydrogen adsorption vs the fraction of the platinum surface covered are shown in Fig. 3. Each of the plot segments corresponds to a gas addition in run Nos. 1, 4, or 5. The data, together

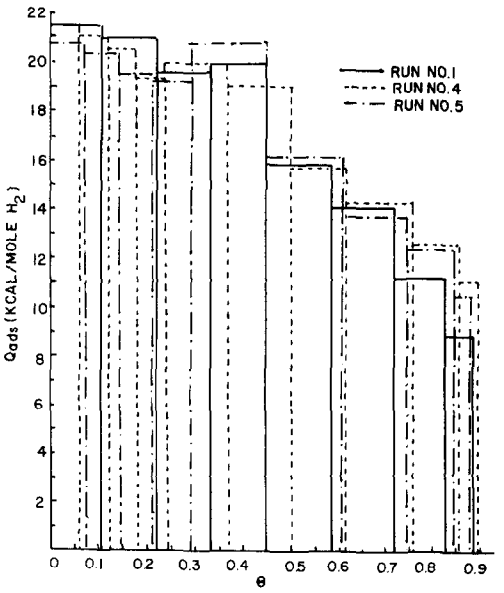

FIG. 3. Heats of hydrogen adsorption vs surface coverage.

TABLE 3

Adsorption and Calorimetric Data for Run No. 4

Adsorption temperature (°K)	Adsorption segment notation	Adsorption segment number	Equilibrium pressure, $P_{eq\,m}$, $P_{eq\,0}$, or $P_{eq,n}$ (Torr)	Amount of hydrogen adsorbed, N_m, N_0, or N_n (μmol)	Uncorrected calorimeter displacement, $D_f - D_i$ (μl)	Average calorimeter drift rate, D (nl/min)	Thermal settling time, t (min)	Adsorption heat, Q_{ads} (kcal/mol)	Fraction of surface covered, θ_m
300	m	1	low	58.1 ± 0.3	4.93	0.36 ± 0.36	209	21.4	0.059
300	m	2	low	60.3 ± 0.3	4.95	[a]	207	21.0	0.119
300	m	3	low	57.5 ± 0.3	4.60	0.08 ± 0.08	191	20.5	0.177
300	m	4	low	60.5 ± 0.3	4.87	0.26 ± 0.12	269	19.3	0.238
300	m	5	low	129.4 ± 0.5	10.14	0.46 ± 0.34	251	19.9	0.368
300	m	6	low	125.8 ± 0.5	8.28	−0.18 ± 0.18	278	19.0	0.495
300	m	7	low	119.3 ± 0.4	7.35	0.26 ± 0.04	197	15.7	0.615
300	m	8	1.0	140.7 ± 0.9	7.83	0.14 ± 0.08	121	14.2	0.757
300	m	9	14.3	95.6 ± 1.0	4.76	0.20 ± 0.20	248	12.6	0.853
300	m	10	47.8	40.0 ± 1.1	1.72	[a]	161	11.1	0.893
210	0	0	19.8	85.4 ± 1.3					
210	n	1	45.1	17.2 ± 1.8					
210	n	2	52.3	4.5 ± 2.3					

[a] Too small to be measured properly.

with the estimated uncertainties, are listed in Tables 2–4. Run Nos. 2 and 3 are not included because bare sections in the diphenylether mantle were observed after these runs were completed. It should be mentioned however, that they were not significantly different from the data shown in Fig. 3 (run No. 4).

All the plots show the characteristic decreases in adsorption heats with increasing surface coverage except for maxima in all three cases. We do not consider the slight decrease in the heat of adsorption with decreasing dispersion to be significant. We feel that the heterogeneity of the surface with respect to the adsorption of hydrogen is not a strong function of dispersion. This may well account for the facile nature of most catalytic hydrogenations over supported platinum and supports the idea that

TABLE 4

Adsorption and Calorimetric Data for Run No. 5

Adsorption temperature (°K)	Adsorption segment notation	Adsorption segment number	Equilibrium pressure, $P_{eq,m}$, $P_{eq,0}$, or $P_{eq,n}$ (Torr)	Amount of hydrogen adsorbed, N_m, N_0, or N_n (μmol)	Uncorrected calorimeter displacement, $D_f - D_i$ (μl)	Average calorimeter drift rate, D (nl/min)	Thermal settling time t, (min)	Adsorption heat, Q_{ads} (kcal/mol)	Fraction of surface covered, θ_m
300	m	1	low	56.7 ± 0.3	4.60	0.13 ± 1.06	154	20.7	0.071
300	m	2	low	56.9 ± 0.3	4.70	1.72 ± 0.53	116	20.3	0.143
300	m	3	low	55.4 ± 0.3	4.33	0.51 ± 0.35	233	19.4	0.213
300	m	4	low	61.6 ± 0.3	4.55	−0.32 ± 0.38	223	19.2	0.291
300	m	5	low	127.1 ± 0.5	10.34	0.19 ± 0.13	186	20.8	0.451
300	m	6	low	126.7 ± 0.5	7.98	0.16 ± 0.16	121	16.1	0.610
300	m	7	1.4	107.1 ± 0.8	5.82	1.09 ± 0.48	71	13.7	0.745
300	m	8	20.1	78.9 ± 1.0	3.82	[a]	399	12.4	0.845
300	m	9	29.6	25.7 ± 1.1	1.05	[a]	127	10.5	0.877
210	0	0	22.1	81.4 ± 1.3					
210	n	1	45.7	13.2 ± 1.9					
210	n	2	52.1	4.4 ± 2.3					

[a] Too small to be measured properly.

chemisorbed hydrogen may be quite mobile over the metal (*18*).

One might speculate that the occurrence of maxima in the heat of adsorption plots might conceivably be due to different species of chemisorbed hydrogen. Rootsaert *et al.* (*19*) found from field emission studies on a clean platinum surface that two types of hydrogen exist: a strongly adsorbing type with a negative surface potential and a weaker one with a positive surface potential. This information was obtained from a hydrogen desorption experiment, in which a large negative maximum in surface potential occurred at −30°C as the temperature was increased. This maximum was assumed to indicate that as the weaker, positive hydrogen desorbed first, the surface potential became more negative. As the maximum was reached, desorption of the more stable, negative type began to dominate. This maximum corresponded to a surface coverage of about 40%, within the region of the maxima in Fig. 3. In this work, the hydrogen was adsorbed at 77°K in contrast to the present study. Tsuchiya *et al.* (*20*) found that most of the adsorbed hydrogen desorbed from a platinum-black catalyst in two very distinct temperature regions, −20 and 90°C when the temperature was raised linearly from −76 to 500°C. These results also apparently confirm the existence of at least two different kinds of hydrogen.

No precedent exists in the literature for maxima in heat of adsorption plots for hydrogen adsorbed on platinum; however, one must also consider less elegant explanations for this phenomenon. According to Gravelle (*21*), gas diffuses very slowly through a large quantity of powdered catalyst, causing some portions to be shielded. If adsorption is not completely reversible, incoming adsorbate will actually bond first to less energetic sites near the surface of the catalyst bed and not redistribute to some of the more energetic sites deep within it. Hydrogen may thus adsorb at some of these more energetic sites at apparently higher fractional surface coverages than would be expected.

The role of the chloride contamination is not known; however, chloride contamination is almost always present when chloroplatinic acid solutions are used in impregnating solutions. Wilson and Hall (*22*) have found a promotional enhancement in the rate of deuterium hydroxyl exchange in the presence of chloride. Presumably, the chloride ion enables adsorbed hydrogen atoms to migrate to the support more readily. In the present study, chloride ions were removed by each progressive heat treatment. Since initial heats of adsorption were rather insensitive to dispersions, we do not think that chloride contamination is a serious factor.

In conclusion, we feel that calorimetric studies support data in the literature which show that a large majority of catalytic hydrogenations over supported platinum are facile.

ACKNOWLEDGMENTS

We wish to acknowledge the financial aid obtained from the Petroleum Research Fund, from which both a fellowship and research support were granted, as well as the support from the United States Government in the form of an N.D.E.A. Fellowship.

REFERENCES

1. Taylor, H. S., *Proc. Roy. Soc.* (*London*), *Ser. A* **108**, 105 (1925; also, *J. Phys. Chem.* **30**, 145 (1926).
2. Poltorak, O. M., and Boronin, V. S., *Russ. J. Phys. Chem.* (*Transl.*) **40**, 1436 (1966).
3. Boudart, M., Aldag, A., Benson, J. E., Dougharty, N. A., and Haskins, C. G., *J. Catal.* **6**, 92 (1966).
4. Boudart, M., Aldag, A. W., Ptak, L. D., and Benson, J. E., *J. Catal.* **11**, 35 (1968).
5. Van Hardeveld, R., and Van Montfoort, A., *Surface Sci.* **4**, 396 (1966).
6. Boronin, V. S., Nikulina, V. A., and Poltorak, O. M., *Vestn. Mosk Univ., Khim.* **13**, 270 (1972).
7. Bond, G. C., "Catalysis by Metals," pp. 74–86. Academic Press, New York, 1962.
8. Bradley, R. S., *J. Sci. Instrum.* **31**, 129 (1954).

9. Jessup, R. S., *J. Res. Nat. Bur. Stand.* **55**, 317 (1955).
10. Shanefield, D., *Rev. Sci. Instrum.* **32**, 1403 (1961).
11. Lantz, Joel B., Ph.D. thesis, University of Rhode Island, 1974.
12. Dainton, F. S., Diaper, J., Ivin, K. J., and Sheard, D. R., *Trans. Faraday Soc.* **53**, 1269 (1957).
13. Boronin, V. S., Nikulina, V. S., and Poltorak, O. M., *Russ. J. Phys. Chem. (Transl.)* **37**, 626 (1963).
14. Dorling, T. A., Lynch, B. W. J., and Moss, R. L., *J. Catal.* **20**, 190 (1971).
15. Kung, H. H., Brookes, B. I., and Burwell, R. L., Jr., *J. Phys. Chem.* **78**, 875 (1974).
16. Vannice, M. A., Benson, J. E., and Boudart, M., *J. Catal.* **16**, 348 (1970).
17. Spenadel, L., and Boudart, M., *J. Phys. Chem.* **64**, 205 (1960).
18. Vannice, M. A., private communication.
19. Rootsaert, W. J. M., Van Reijen, L. L., and Sachtler, W. M. H., *J. Catal.* **1**, 416 (1962).
20. Tsuchiya, S., Amenomiya, Y., and Cvetanovic, R. J., *J. Catal.* **19**, 245 (1970).
21. Gravelle, P. C., *Advan. Catal.* **22**, 191 (1972).
22. Wilson, G. R., and Hall, W. K., *J. Catal.* **17**, 190 (1970).